Optimization and coordination of SVC-based supplementary controllers and PSSs to improve power system stability using a genetic algorithm

Ali Darvish FALEHI∗**, Mehrdad ROSTAMI, Aref DOROUDI**
Abdulaziz ASHRAFIAN
Department of Electrical Engineering, Shahed University, Tehran-IRAN
e-mail: darvishfalehi@shahed.ac.ir

Abstract

In this paper, a lead-lag structure is proposed as a main damping controller for a static VAR compensator (SVC) to diminish power system oscillations. To confirm the transient performance of the proposed controller, it was compared to a proportional integral derivative (PID) damping controller. Power system stability improvement was thoroughly examined using these supplementary damping controllers as well as a power system stabilizer (PSS). The generic algorithm (GA) is well liked in the academic environment due to its immediate perceptiveness, ease of performance, and ability to impressively solve highly nonlinear objectives. Thus, the GA optimization technique was applied to solve an optimization problem and to achieve optimal parameters of the SVC-based supplementary damping controllers and PSS. The coordinated design problem of these devices was formulated as an optimization problem to reduce power system oscillations. The transient performance of the damping controllers and PSS were evaluated under a severe disturbance for a single-machine infinite bus (SMIB) and multimachine power system. The nonlinear simulation results of the SMIB power system suggest that power system stability was increasingly improved using the coordinated design of the SVC-based lead-lag controller and PSS, rather than the coordinated design of the SVC-based PID controller and PSS. Furthermore, the interarea and local modes of the oscillations were superiorly damped using the proposed controller in the multimachine power system.

Key Words: *SVC, PSS, power system stability, coordinated design, lead-lag damping controller, PID damping controller, GA optimization technique*

1. Introduction

Recent advances in the field of power electronics pave the way to use of flexible alternating current transmission system (FACTS) devices in power systems. FACTS devices are able to control the network status in very rapid events and, because of this, increase the transient stability of the power system. Shunt FACTS devices with

---

∗Corresponding author: Department of Electrical Engineering, Shahed University, Tehran-IRAN

compensating reactive power capability play an important role in controlling active power through the power network, mitigating voltage fluctuations, and increasing transient stability in power systems [1,2].

Power system stabilizers (PSSs) are one of the most common controllers designed to increase damping of electromechanical oscillations, and they have been used for many years [3]. They are also used to compensate for the negative damping of automatic voltage regulators (AVRs) [4]. PSSs give a modulating signal through the excitation system to damp out rotor oscillations. However, under some operating conditions, PSSs may not function properly, particularly in the damping of interarea oscillating modes [5-7].

In current applications, FACTS technology appears as a suitable choice to damp electromechanical oscillations, along with critical bus voltage amplitudes and phase angles. A static VAR compensator (SVC) is a shunt FACTS device that is more common and is widely used in power networks, as it has the capability of increasing steady-state capacity and enhancing the dynamic performance and transient stability of power systems.

Different techniques and controllers have been presented to improve transient stability and reduce power system oscillations using FACTS devices [8-11]. The prototypes of 2 shunt FACTS devices, a thyristor-switched reactor (TSR)-based SVC and a thyristor-controlled reactor (TCR)-SVC, were developed in [12]. FACTS devices have also been employed as modern devices to damp the undesired swings in power systems [13,14]. Furthermore, the optimum location of FACTS devices on transmission lines have been studied, taking into consideration power system stability, power losses, and the maximum capability of the power transfer [15-19].

A number of conventional techniques have been applied to implement power system stabilizers, including mathematical programming, gradient processes, and modern control theories [20]. However, the use of conventional techniques has a few disadvantages, such as heavy computations and slow convergence. In addition, the search process is sensitive and may be trapped in local minima. The progressive methods search for the optimum solutions via some sort of directed random search processes. A suitable feature of the evolutionary methods is searching for the optimal solutions without prior problem perception. In recent years, computation techniques based on genetic algorithms (GAs) have been applied as an optimization tool in various probe areas, such as the design of controllers [21], improvement of the voltage profile of a self-excited induction generator [22], and optimum placement of FACTS devices [23-27]. GAs have been used to design the FACTS controllers for damping of power system oscillations and enhancement of power system stability [28,29].

The proportional integral derivative (PID) controller, due to its functional simplicity and predictability, is successfully employed in industrial applications [30]. It has also been used as a supplementary controller for FACTS devices to damp power system oscillations [31,32]. In [33], for damping the low-frequency oscillation, 2 kinds of controllers, a lead-lag and a PID controller, were applied to a thyristor-controlled series compensator (TCSC). That paper showed that the lead-lag structure was more effective than the PID controller.

In this paper, a lead-lag structure is proposed as the main damping controller for a SVC to reduce the low-frequency oscillations in a power system. The proposed controller is compared with a PID controller. A GA optimization technique is applied to coordinate the SVC-based damping controller and the PSS in order to improve the stability of the power system. The transient performance of both damping controllers and the PSS are evaluated under a severe disturbance in a single-machine infinite bus (SMIB) and in a multimachine network. Simulation results of the SMIB power system suggest that the stability of the power system is improved using the coordinated design of the SVC-based lead-lag controller and PSS. Moreover, the interarea and local modes of the oscillations are superiorly damped using this controller in a multimachine power system.

2. SMIB power system model with SVC-based damping controllers and a PSS

2.1. System model

The single-line diagram of the SMIB system and its model using MATLAB/Simulink software (MathWorks, Natick, MA, USA) are shown in Figures 1 and 2, respectively. The power system comprised a synchronous generator connected to an infinite bus through a step-up transformer, followed by a double circuit transmission line. The generator was equipped with a hydraulic turbine and governor (HTG), excitation system, and PSS. The SVC was connected to the sending bus as shown in Figure 1. All of the relevant parameters are given in Appendix A.1.

Generally, a SVC is made of a TCR and a TSC bank, and it is connected parallel to the network [2]. A SVC acts as a variable reactance to maintain or control some power system variables, typically bus voltages [10]. It is used extensively for fast reactive power generation and voltage regulation. A power system equipped with a SVC can improve dynamic voltage control, increase the load carrying capacity, and enhance the stability of the power system. The PSS acts through the excitation system of the generator, providing additional damping torque proportional to the speed change [34].
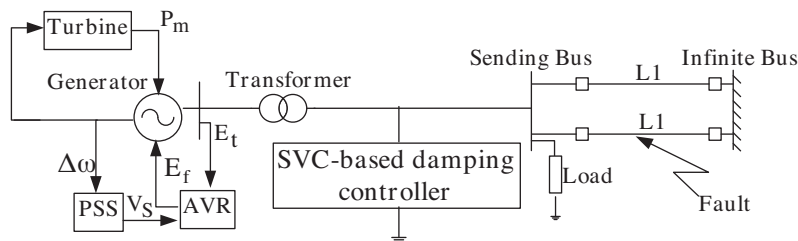

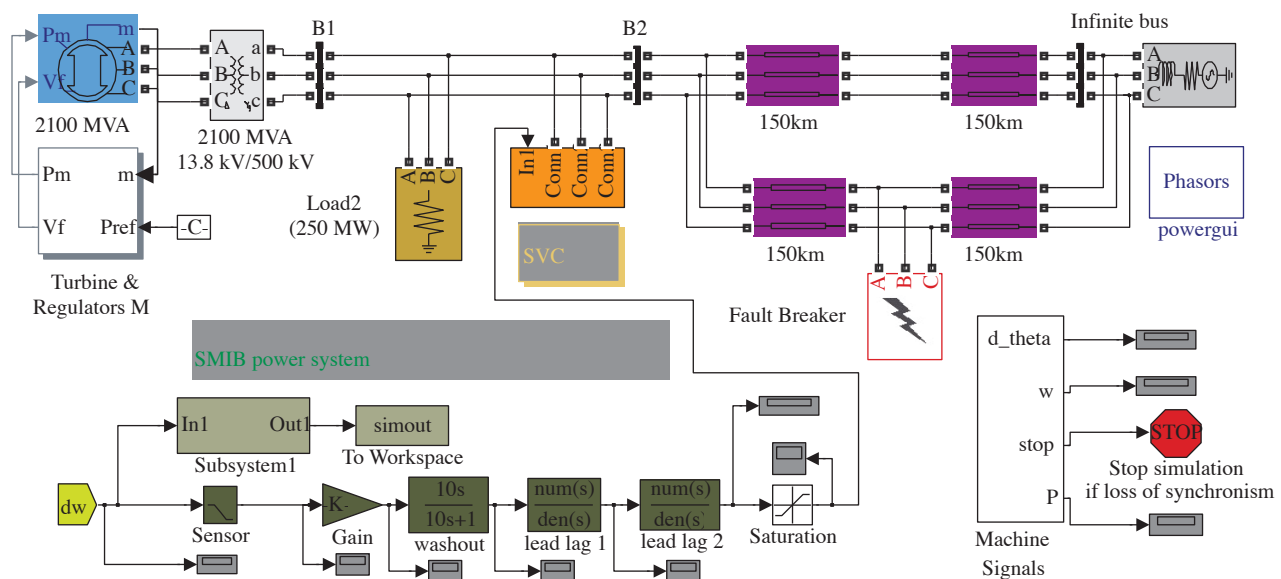**Figure 1.** Single-line diagram of the SMIB power system with a SVC.

Figure 2. MATLAB simulation model of the SMIB power system with a SVC.

2.2. Structure of the SVC-based lead-lag damping controller

The SVC-based lead-lag damping controller is shown in Figure 3. The device uses a lead-lag structure and acts as a controller to regulate the SVC voltage signal (V_S). The structure includes a gain block (with gain K_S), a signal washout block, and 2 first-order phase compensation blocks. The phase-compensation block provides the proper phase-lead characteristics to compensate for the phase lag between the input and output signals. The signal washout block is a high-pass filter with the time constant T_{WS}, high enough to allow the input signal to pass unchanged. Without it, steady changes in speed would modify the Vs. It allows the controller to respond only to changes in speed.
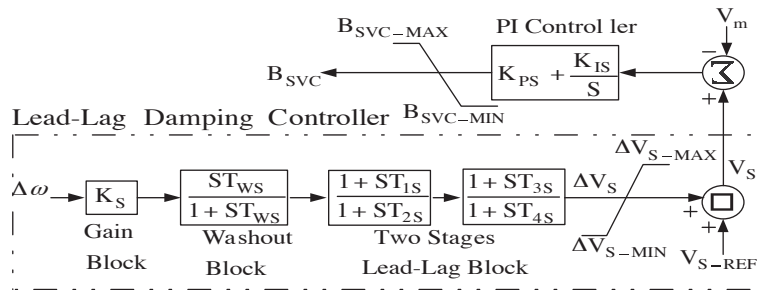

Figure 3. Structure of the SVC-based lead-lag damping controller.

2.3. Structure of the SVC-based PID damping controller

The SVC-based PID damping controller is shown in Figure 4. The device uses a PID structure as a controller to regulate the SVC V_S. The structure includes a proportional block with gain K_{Pd}, an integral block with gain K_{Id}, and a derivative block with gain K_{Dd}. A supplementary PID damping controller generates the signal from the generator speed deviation to improve the stability of the power system.
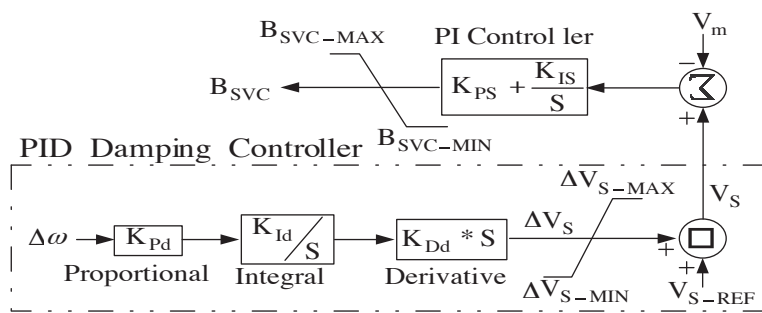

Figure 4. Structure of the SVC-based PID damping controller.

2.4. Structure of the power system stabilizer

The PSS includes an amplification block, a signal washout block, a lead-lag block, and a sensor delay block [4,10,20,28]. The lead-lag block provides a proper phase-lead characteristic to compensate for the phase lag between the generator electrical torque and the exciter input. The PSS input signal can be either speed deviation or active power. The structure of the PSS controller is presented in Figure 5.
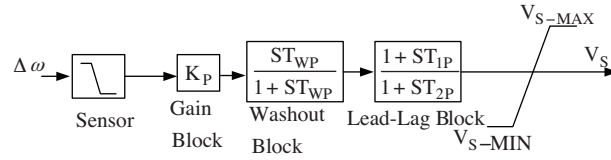
Figure 5. Structure of the PSS.

2.5. Problem formulation

From the viewpoint of the washout function, the value of T_w is not critical and may be in the range of 1-20 s. The main consideration is that it be long enough to pass stabilizing signals at the frequencies of interest unchanged [4]. In this paper, the values of T_{WS} and T_{WP} were considered to be 10 and 3, respectively. The sensor delay time was assumed to be 15 ms. The other parameters that should be optimized were as follows:

- Lead-lag controller: gain (K_S) and time constants (T_{1S}, T_{2S}, T_{3S}, and T_{4S}).

- PID controller: proportional gain (K_{Pd}), integral gain (K_{Id}), and derivative gain (K_{Dd}).

- AC-voltage PI-controller: proportional gain (K_{PS}) and integral gain (K_{IS}).

- PSS: gain (K_P) and the time constants (T_{1P} and T_{2P}).

During steady-state conditions, ΔV_S and V_{S-ref} are constant. In dynamic operations (oscillations), V_S is adjusted to damp system oscillations. The value of V_S in this condition is determined by:

$$V_S = V_{S-ref} + |\Delta V_S. \tag{1}$$

The value of susceptance can be expressed as:

$$(V_S - V_m)(K_{PS} + K_{IS}/S) = B_{SVC}, \tag{2}$$

where V_m is the linear mean value of the SVC bus voltage.

In the present study, the integral time absolute error (ITAE) of the speed signal deviation was considered as the objective function J:

$$J = \int_{t=0}^{t=t_{sim}} |\Delta\omega|.t.dt, \tag{3}$$

where $\Delta\omega$ is the speed signal deviation and t_{sim} is the simulation time.

The time-domain simulation of the nonlinear system model was performed to minimize the above objective function in order to improve the system response based on settling time, overshoots, and undershoots. The constraints were the PSS and SVC controller parameter bounds. The problem can be formulated as the optimization procedure below.

$$\text{Minimize} J \tag{4}$$

Subject to

$$K_S^{\min} \leq K_S \leq K_S^{\max} \quad K_{Dd}^{\min} \leq K_{Dd} \leq K_{Dd}^{\max}$$
$$T_{1S}^{\min} \leq T_{1S} \leq T_{1S}^{\max} \quad K_{PS}^{\min} \leq K_{PS} \leq K_{PS}^{\max}$$
$$T_{2S}^{\min} \leq T_{2S} \leq T_{2S}^{\max} \quad K_{IS}^{\min} \leq K_{IS} \leq K_{IS}^{\max}$$
$$T_{3S}^{\min} \leq T_{3S} \leq T_{3S}^{\max} \quad K_{Pi}^{\min} \leq K_{Pi} \leq K_{Pi}^{\max}, \text{for single-machine} i = 1 \tag{5}$$
$$T_{4S}^{\min} \leq T_{4S} \leq T_{4S}^{\max} \quad T_{1Pi}^{\min} \leq T_{1Pi} \leq T_{1Pi}^{\max}, \text{for multimachine} i = 1, 2, \ldots, n$$
$$K_{Pd}^{\min} \leq K_{Pd} \leq K_{Pd}^{\max} \quad T_{2Pi}^{\min} \leq T_{2Pi} \leq T_{2Pi}^{\max}, n = \text{ number of } PSSs$$
$$K_{Id}^{\min} \leq K_{Id} \leq K_{Id}^{\max}$$

Traditional optimization methods are not reliable for obtaining optimal controller parameters in multi-mode conditions and they are sometimes based on trial and error. Modern intelligent optimization techniques use time-domain simulation and optimize the objective function for tuning parameters. Furthermore, the effect of time-domain constraints can be simply applied. In this paper, the GA technique was used to solve the above optimization problem.

3. Genetic algorithm

The GA is a good candidate for solving nonlinear problems because of its superior robust behavior in nonlinear circumference over mixing optimization techniques. GAs are usually more flexible and robust than other methods, and they have been successfully used in power system planning [35]. In this paper, the optimized parameters of the SVC-based supplementary damping controllers and PSSs were obtained by applying the GA. The process of the GA optimization technique can be explained as follows:

Step 1: Inputs of the GA technique are the population size and the maximum number of a generation. Moreover, the crossover and mutation methods and those probabilities should first be specified for probability.

$$\text{chromosome (variables)} = [P_1, P_2, ..., P_{Nvar}] \tag{6}$$

$$\text{cost} = f(\text{chromosome}) = f(P_1, P_2, ..., P_{Nvar}) \tag{7}$$

Here, N_{var} is the total number of different variables.

Step 2: Subsequently, considering the variables' length limitations, the initial population is randomly generated. Each of the chromosomes (genes) represents a possible solution of the optimization problem.

$$p = (p_{hi} - p_{lo})p_{norm} + p_{lo} \tag{8}$$

Here, p_{lo}, p_{hi}, and p_{norm} are the highest number in the variable range, the lowest number in the variable range, and the normalized value of the variable, respectively.

Step 3: After the initial population of the GA is generated, the objective function is appointed as the fitness of the GA.

Step 4: The genetic operations are selection, crossover, and mutation. To continue the generation, selection of the individuals plays a very important role in the GA. The selection function determines which of the individuals will survive and move on to the next generation. Crossover occurs expressed as the following parameter:

$$\alpha = \text{ roundup } \{\text{random} * Nvar\}. \tag{9}$$

Each pair of mates creates a child bearing some mix of the 2 parents.

$$\text{parent } 1 = [p_{m1}p_{m2}...p_{m\alpha}...p_{mNvar}],$$

$$parent2 = [p_{d1}p_{d2}...p_{d\alpha}...p_{dNvar}]. \tag{10}$$

Here, the m and d subscripts discriminate between the "mom" and the "dad" parent. The selected variables are thus combined to form new variables that will appear in the children:

$$p_{new1} = p_{m\alpha} - \beta[p_{m\alpha} - p_{d\alpha}],$$

$$p_{new2} = p_{d\alpha} + \beta[p_{m\alpha} - p_{d\alpha}], \tag{11}$$

where β is also a random value between 0 and 1. The final step is to complete the crossover with the rest of the chromosomes as before:

$$offspring\_1 = [p_{m1}p_{m2}...p_{new1}...p_{dNvar}],$$

$$ofspring\_2 = [p_{d1}p_{d2}...p_{new2}...p_{mNvar}]. \tag{12}$$

Crossover is the core of the genetic operation, which helps to achieve new regions in the search space using a randomized process of swapping information between individuals.

Mutation is usually considered as an auxiliary operator to extend the search space and causes release from a local optimum when used cautiously with the selection and crossover systems. By adding a normally distributed random number to the variable, uniform mutation will be obtained:

$$p_n' = p_n + \sigma N_n(0,1), \tag{13}$$

where σ = standard deviation of the normal distribution, and $N_n(0,1)$ = standard normal distribution (mean = 0 and variance = 1).

Step 5: Operations of selection, crossover, and mutation are repeated until a favorable number of individuals for the new generation is created, and the objective function is calculated again for all of the individuals in the new generation. The best individual in the new generation according to its fitness is kept to continue to the next generation. Thus, the fitness of the entire population will be decreased with the reproduction of the generation.

Step 6: The stopping scale is the maximum number of the generation. The flowchart of the proposed optimization algorithm is shown in Figure 6.

3.1. Simulation results of the SMIB power system with both the lead-lag and PID damping controllers and PSS

To assess the coordinated control between the SVC-based supplementary (lead-lag and PID) damping controllers and PSS, 3 different operating conditions with different fault clearing times (FCTs) were considered and are shown in Table 1.
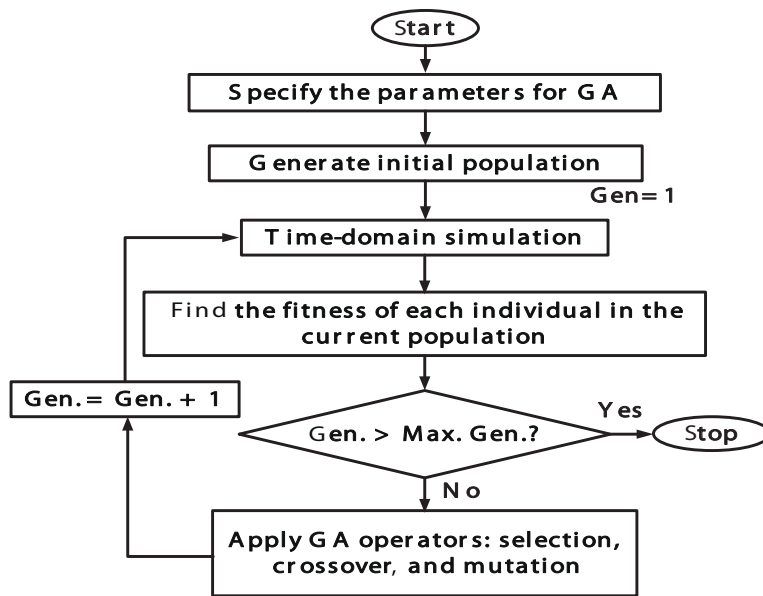
Figure 6. Flowchart of the GA processes for optimization of the controller parameters.

3.2. State-1: Nominal loading

A severe disturbance (3-phase fault) was considered in the middle of the transmission line, at t = 0.1 s, and then cleared after 0.463 s (FCT = 0.463 s).

Using the GA optimization technique, coordinated control between the SVC-based lead-lag damping controller and PSS, and also the SVC-based PID damping controller and PSS, was performed. Subsequently, the optimal controller parameters that were achieved are presented in Tables 2 and 3. The convergence of objective function J is also shown in Figure 7.

The system response under such a severe disturbance is presented in Figures 8-12, which indicate that coordinating the SVC-based lead-lag damping controller and PSS significantly enhanced the stability of the power system compared with other cases. Nonoptimum parameters of the PSS and AC-voltage PI-controller can be found in [4] and [36], respectively.

Table 1. Three different operating conditions.

| Loading conditions	P_e per unit (pu)	δ_0 (deg)	FCT (s)
Light	0.35	19.6	0.412
Nominal	0.7	42.2	0.463
Heavy	0.95	58	0. 166

Table 2. Optimal parameter settings of the PSS and SVC-based lead-lag damping controller.

| SVC AC-voltage PI controller-based lead-lag damping controller							PSS		
PI controller		Supplementary lead-lag damping controller							
K_{PS}	K_{IS}	K_S	T_{1S}	T_{2S}	T_{3S}	T_{4S}	K_P	T_{1P}	T_{2P}
4.2005	2.3213	232.1883	0.6089	0.8382	0.2597	0.3859	3.1477	0.0746	0.8540

Table 3. Optimal parameter settings of the PSS and SVC-based PID damping controller.

| SVC AC-voltage PI controller-based PID damping controller | | | | | PSS | | |
PI controller		Supplementary PID damping controller					
K_{PS}	K_{IS}	K_{Pd}	T_{Id}	T_{Dd}	K_P	T_{1P}	T_{2P}
3.1008	2.1231	61.5188	0.3101	0.0972	7.2510	0.0319	1.1703
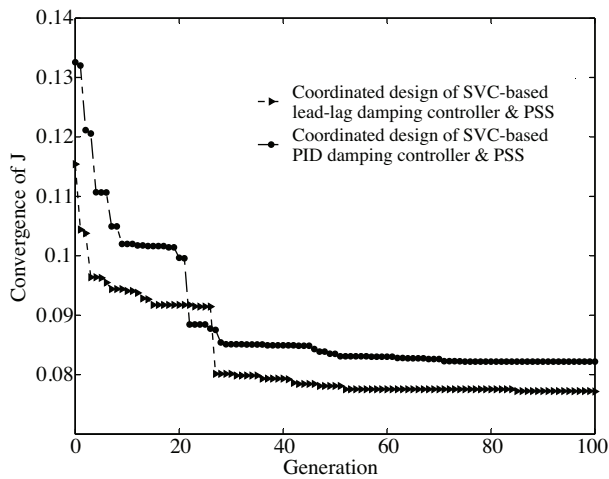
**Figure 7.** Convergence of the objective function.
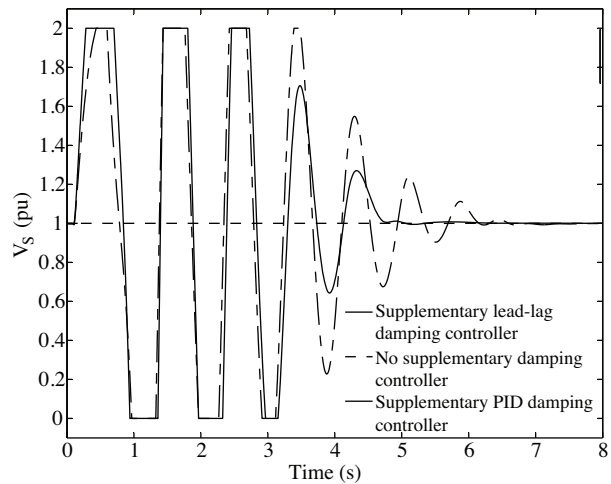
Figure 8. Variation of the SVC reference voltage signal under a 3-phase fault in the transmission line with nominal loading.
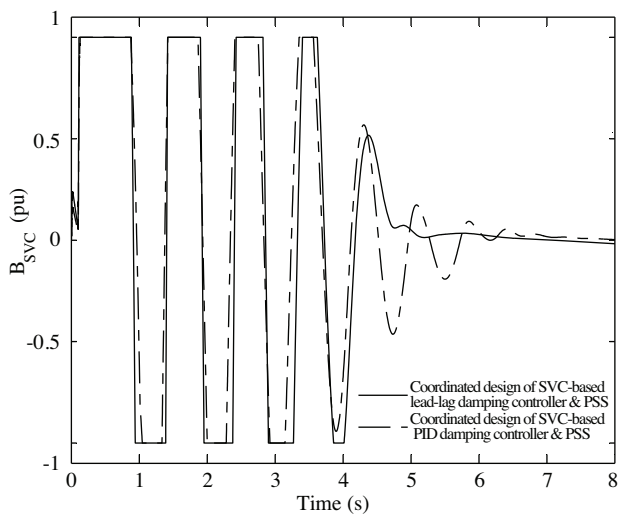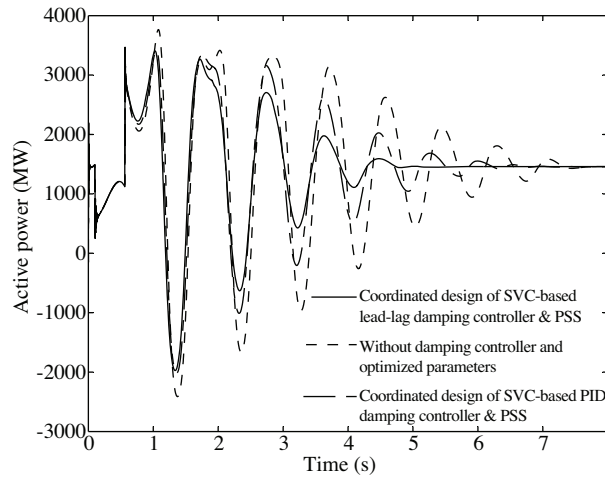

Figure 9. Variation of the SVC susceptance under a 3-phase fault in the transmission line with nominal loading.
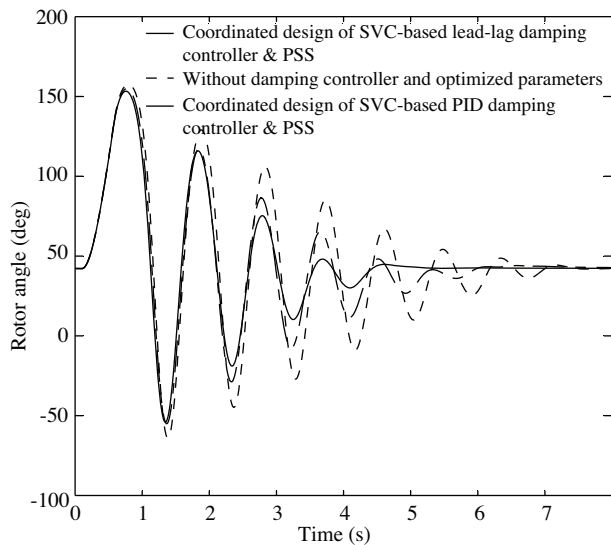
Figure 10. Variation of the rotor angle under a 3-phase fault in the transmission line with nominal loading.

647
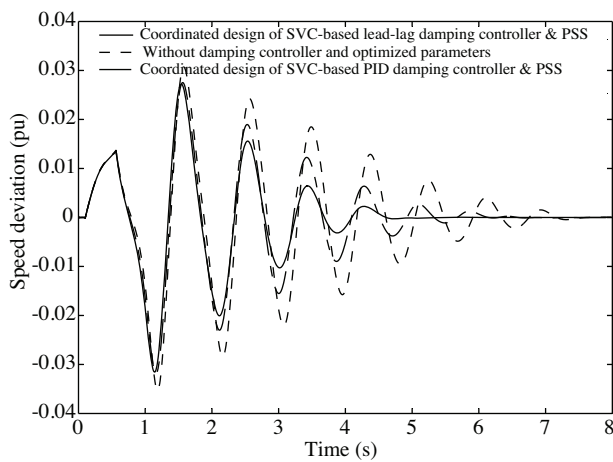
Figure 11. Variation of the speed deviation under a 3-phase fault in the transmission line with nominal loading.


Figure 12. Variation of sending-end active power from bus-1 under a 3-phase fault in the transmission line with nominal loading.

3.3. State-2: Heavy loading

In this state, to evaluate the coordinated design of these devices, generator loading was set at heavy loading, as shown in Table 1. In addition, the location of the 3-phase fault was considered on bus-3. The 3-phase fault occurs at $t = 0.1$ s, and the fault was cleared after 0.166 s. System response under the 3-phase fault is displayed in Figure 13. Obviously, coordinating the SVC-based lead-lag damping controller and PSS resulted in significantly improved stability of the power system compared to the coordinated design of the SVC-based PID damping controller and PSS as well as the nonoptimized parameters of these devices.
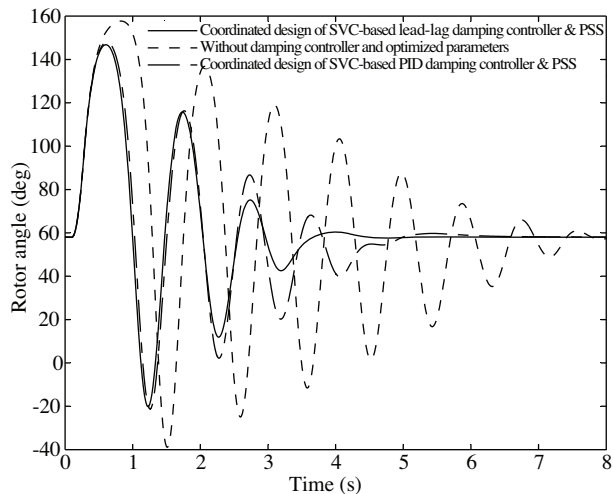
Figure 13. Variation of the rotor angle under a 3-phase fault in the transmission line with heavy loading.
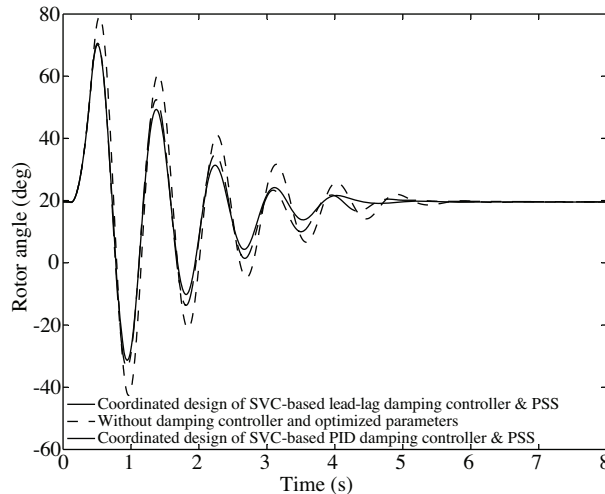
Figure 14. Variation of the rotor angle under a 3-phase fault in the transmission line with light loading.

3.4. State-3: Light loading

For this case, the generator loading was altered to small loading, as shown in Table 1. In addition, a 3-phase short circuit occurred in bus-1 at $t = 0.1$ s and was subsequently cleared after 0.412 s. System response under

such a disturbance is displayed in Figure 14. As can be seen, the stability of the power system was superiorly improved by the coordinated control between the SVC-based lead-lag damping controller and the PSS.

4. Multimachine power system with lead-lag and PID damping controllers and PSSs

4.1. System model

A single-line diagram of the 3-machine, 2-area power system model is shown in Figure 15. The system is almost similar to the power system used in [35,37,38]. The speed of generators G1 and G3 were chosen as the input signal of both the lead-lag and PID damping controllers. It was assumed that the SVC was located between bus-5 and bus-6. All 3 of the generators were equipped with a PSS, a HTG, and an excitation system. All of the relevant parameters are given in Appendix A.2.
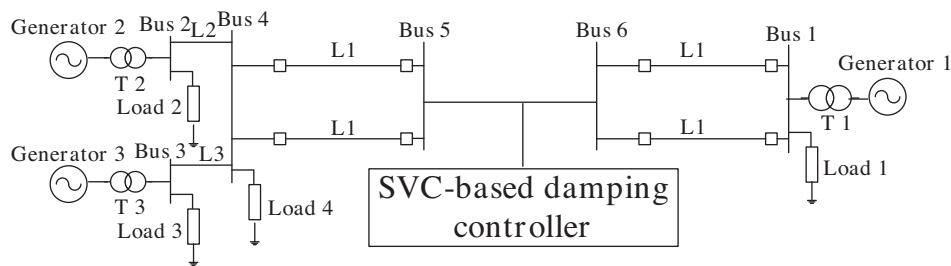
Figure 15. Single-line diagram of a 3-machine, 2-area power system with a SVC.

Objective function J was determined as follows:

$$J = \int_{t=0}^{t=t_{sim}} (|\omega_1 - \omega_2| + |\omega_3 - \omega_2|).t.dt, \tag{14}$$

where ω_1, ω_2, and ω_3 are the speeds of generators G_1, G_2, and G_3, respectively, and t_{sim} is the time range of the simulation. The oscillations between generators G_2 and G_3 are local modes of oscillation. Moreover, the oscillations between generators G_2 and G_1 or between G_1 and G_3 are interarea modes of oscillation in the presented power system. Generally, the frequency of multimode oscillation is composed of 3 major modes: interarea mode 0.2-0.8 Hz, local mode 0.8-1.5 Hz, and interplant mode 1.5-2.5 Hz [39].

5. Simulation results

To evaluate the coordinated control between the SVC-based supplementary damping controller and the PSS, a 3-phase fault was triggered on bus-1 at t = 0.1 s and then cleared in 0.299 s. As described above, the GA optimization technique was employed to acquire the coordinated control between the SVC-based lead-lag damping controller and the PSSs, and also between the SVC-based PID damping controller and PSSs. Subsequently, the parameters of these devices were optimally tuned in order to damp the power system oscillations. The optimal parameters of the SVC-based damping controller and PSSs to obtain more than 50 generations are tabulated in Tables 4 and 5.

The system's response under this disturbance is presented in Figures 16-18. These results proved that by the coordination of the SVC-based lead-lag damping controller and PSSs, the stability of the power system was significantly improved compared to the noncoordinated criteria and coordination of the SVC-based lead-lag damping controller and PSSs.
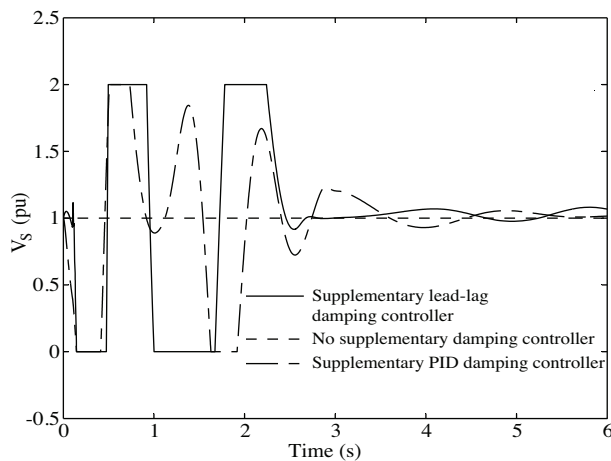
The variations of the interarea and local modes of oscillations are presented in Figures 17 and 18, respectively. Obviously, without the damping controller or optimized parameters, both the interarea and the local modes of oscillations were extremely oscillatory. However, these modal oscillations were significantly damped out by the coordination of the lead-lag damping controller and PSSs, even more so than with the PID damping controller and PSSs.

Table 4. Optimal parameter settings of the PSSs and SVC-based lead-lag damping controller.

SVC AC-voltage PI controller-based lead-lag damping controller						
PI controller		Supplementary lead-lag damping controller				
K_{PS}	K_{IS}	K_S	T_{1S}	T_{2S}	T_{3S}	T_{4S}
0.8772	4.9417	241.8878	0.9881	0.0529	0.0922	0.5535
PSSs						
PSS-1			PSS-2			PSS-3		
K_{P1}	T_{1P1}	T_{2P1}	K_{P2}	T_{1P2}	T_{2P2}	K_{P3}	T_{1P3}	T_{2P3}
2.4112	0.2444	0.6975	1.7906	0.9780	0.8586	1.4867	1.8103	1.5925

Table 5. Optimal parameter settings of the PSSs and SVC-based PID damping controller.

SVC AC-voltage PI controller-based lead-lag damping controller						
PI controller		Supplementary lead-lag damping controller				
K_{PS}	K_{IS}	K_S	T_{1S}	T_{2S}	T_{3S}	T_{4S}
0.8772	4.9417	241.8878	0.9881	0.0529	0.0922	0.5535
PSSs						
PSS-1			PSS-2			PSS-3		
K_{P1}	T_{1P1}	T_{2P1}	K_{P2}	T_{1P2}	T_{2P2}	K_{P3}	T_{1P3}	T_{2P3}
2.4112	0.2444	0.6975	1.7906	0.9780	0.8586	1.4867	1.8103	1.5925

Figure 16. Variation of the SVC reference voltage signal under a 3-phase fault in the transmission line for a 3-machine, 2-area power system.
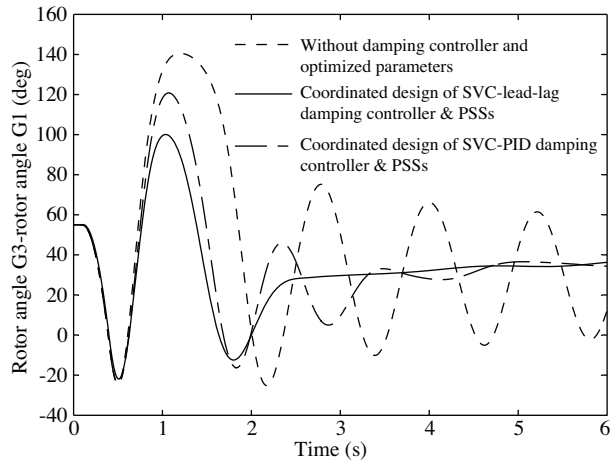
Figure 17. Interarea mode of oscillation under a 3-phase fault in the transmission line.
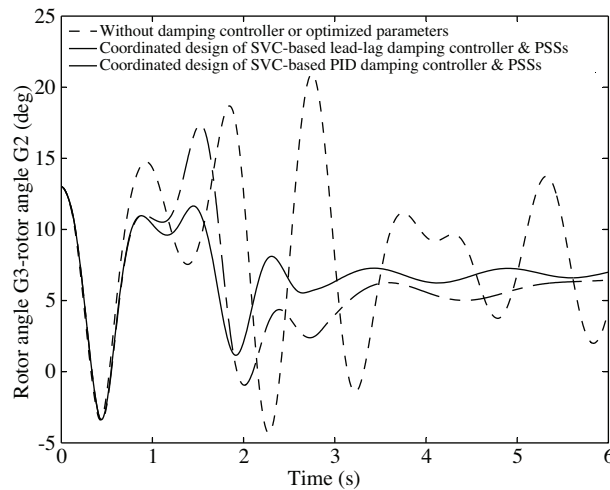
Figure 18. Local mode of oscillation under a 3-phase fault in the transmission line.

6. Conclusion

In this paper, 2 lead-lag and PID structures were proposed as supplementary damping controllers for the SVC to enhance the stability of the power system. To confirm the transient performance of the lead-lag damping controller, it was compared with the PID damping controller. Two types of power systems, a single-machine infinite-bus and a 3-machine, 2-area system, were considered to appraise the coordinated control of the SVC-based damping controller and PSS under a severe disturbance. The GA-optimization technique was employed to tune the parameters of the SVC-based supplementary damping controller and PSS in order to coordinate between the devices optimally.

First, transient stability improvement for the single-machine infinite-bus power system was thoroughly estimated under 3 different operating conditions caused by a 3-phase fault. The results of the simulations suggest that transient stability was dramatically improved by the coordinated design of the SVC-based lead-lag damping controller and PSS compared to the coordinated design of the SVC-based PID damping controller and PSS, and to the noncoordinated criteria.

Finally, the coordinated design problem was applied to the 3-machine, 2-area power system under a severe disturbance. The results showed that with the coordination of the SVC-based lead-lag damping controller and PSS using the GA-optimization technique, the local and interarea modes of oscillations were superiorly damped compared to other cases.

Appendix

A.1. SMIB power system

Generator: $S_B = 2100$ MVA, H = 3.7 s, $V_B = 13.8$ kV, f = 60 Hz, $R_S = 2.8544$e-3, $X_d = 1.305$ pu, $X_d' = 0.296$ pu, $X_d'' = 0.252$ pu, $X_q = 0.474$ pu, $X_q' = 0.243$ pu, $X_q'' = 0.18$ pu, $T_d = 1.01$ s, $T_d' = 0.053$ s, $T_{qo}'' = 0.1$ s.

Load at bus-2: 250 MW.

Transformer: 2100 MVA, 13.8/500 kV, 60 Hz, $R_1 = R_2 = 0.002$ pu, $L_1 = 0$, $L_2 = 0.12$ pu, D_1/Y_g connection, $R_m = 500$ pu, $L_m = 500$ pu.

Transmission line: 3-phase, 60 Hz, Length = 300 km each, R_1 = 0.02546 Ω/km, R_0 = 0.3864 Ω/km, L_1 = 0.9337e-3 H/km, L_0 = 4.1264e-3 H/km, C_1 = 12.74e-9 F/km, C_0 = 7.751e-9 F/km.

Hydraulic turbine and governor: K_a = 3.33, T_a = 0.07, G_{min} = 0.01, G_{max} = 0.97518, $V_{g\,min}$ = –0.1 pu/s, $V_{g\,max}$ = 0.1 pu/s, R_p = 0.05, K_p = 1.163, K_i = 0.105, K_d = 0, Td = 0.01 s, β = 0, T_w = 2.67 s.

Excitation system: T_{LP} = 0.02 s, K_a = 200, T_a = 0.001 s, K_e = 1, T_e = 0, T_b = 0, T_c = 0, K_f = 0.001, T_f = 0.1 s, $E_{f\,min}$ = 0, $E_{f\,max}$ = 7, K_p = 0.

SVC parameters: 500 KV, $\pm$100 MVAR, T_d = 4 ms, injected voltage magnitude limit: V_S = 0-2

Injected SVC susceptance limit: B_{SVC} = $\pm$1 pu.

PSSs: Sensor time constant = 0.015 s, V_S^{max} = 0.15 pu, V_S^{min} = –0.15 pu.

A.2. Multimachine power system

Generators: S_{B1} = 4200 MVA, S_{B2} = S_{B3} = 2100 MVA, V_B = 13.8 kV, f = 60 Hz, X_d = 1.305 pu, X_d' = 0.296 pu, X_d'' = 0.252 pu, X_q = 0.474 pu, X_q' = 0.243 pu, X_q'' = 0.18 pu, T_d = 1.01 s, T_d' = 0.053 s, T_{qo}'' = 0.1 s , R_S = 2.8544e-3, H = 3.7 s, p = 32.

Transformers: S_{B1} = 4200 MVA, S_{B2} = S_{B3} = 2100 MVA, D1/Yg, V_1 = 13.8 kV, V_2 = 500 kV, R_1 = R_2 = 0.002 pu, L_1 = 0, L_2 = 0.12 pu, R_m = 500 pu, L_m = 500 pu.

Transmission lines: 3-phase, R_1 = 0.02546 Ω/km, R_0 = 0.3864 Ω/km, L_1 = 0.9337 e-3 H/km, L_0 = 4.1264 e-3 H/km, C_1 = 12.74 e-9 F/km, C_0 = 7.751 e-9 F/km, L_1 = 175 km, L_2 = 50 km, L_3 = 100 km.

Load 1 = 7500 MW + 1500 MVAR, Load 2 = Load 3 = 25 MW, Load 4 = 250 MW.

References

[1] N.G. Hingorani, L. Gyugyi, Understanding FACTS: Concepts and Technology of Flexible AC Transmission Systems, New York, IEEE Press, 2000.

[2] E. Acha, C.R. Fuerte-Esquiv, H. Ambriz, "Modeling and simulation in power networks", Chichester, Wiley, 2004.

[3] T.R. Jyothsna, K. Vaisakh, "Design of a decentralized non-linear controller for transient stability improvement under symmetrical and unsymmetrical fault condition: a comparative analysis with SSSC", IEEE Power Systems Conference and Exposition, pp. 1-8, 2009.

[4] P. Kunder, Power System Stability and Control, New York, McGraw-Hill, 2001.

[5] J.M. Ramírez, I. Castillo, "PSS and FDS simultaneous tuning", Electric Power Systems Research, Vol. 68, pp. 33-40, 2004.

[6] S. Mishra, "Neural-network-based adaptive UPFC for improving transient stability performance of power systems", IEEE Transactions on Neural Networks, Vol. 17, pp. 461-470, 2006.

[7] E.R. Anarmarzi, M.R. Feyzi, M.T. Hagh, "Hierarchical fuzzy controller applied to multi-input power system stabilizer", Turkish Journal of Electrical Engineering and Computer Sciences, Vol. 18, pp. 541-551, 2010.

[8] L. Angquist, B. Lundin, J. Samuelsson, "Power oscillation damping using controlled reactive power compensation and comparison between series and shunt approaches", IEEE Transactions on Power Systems, Vol. 8, pp. 687-695, 1993.

[9] M. Nooroozian, G. Andersson, "Damping of power system oscillations by use of controllable components", IEEE Transactions on Power Systems, Vol. 9, pp. 2046-2054, 1994.

[10] N. Mithulananthan, C.A. Canizares, J. Reeve, G.J. Rogers, "Comparison of PSS, SVC, and STATCOM controllers for damping power system oscillations", IEEE Transactions on Power Systems, Vol. 18, pp. 786-792, 2003.

[11] N.S. Kurnar, R. Serinivasan, M.A. Khan, "Damping improvement by FACTS device: a comparison between STATCOM, SSSC and UPFC", International Journal of Electrical and Power Engineering, Vol. 2, pp. 171-178, 2008.

[12] A. Gelen, T. Yalçınöz, "Experimental studies of a scaled-down TSR-based SVC and TCR-based SVC prototype for voltage regulation and compensation", Turkish Journal of Electrical Engineering and Computer Sciences, Vol.18, pp. 147-157, 2010.

[13] D. Povh, "Advantages of power electronic equipment in AC system", International Colloquium on HVDC and FACTS Systems, 1993.

[14] G.D. Galanos, "Advanced static compensator for flexible AC transmission", IEEE Transactions on Power Systems, Vol. 8, pp. 113-121, 1993.

[15] Z. Yu, D. Lusan, "Optimal placement of FACTs devices in deregulated systems considering line losses", Electrical Power and Energy Systems, Vol. 26, pp. 813-819, 2004.

[16] S. Panda, R.N. Patel, "Improving power system transient stability with an off-center location of shunt FACTS devices", Journal of Electrical Engineering, Vol. 57, pp. 365-368, 2006.

[17] M.H. Haque, "Optimal location of shunt FACTS devices in long transmission lines", IEE Proceedings - Generation Transmission and Distribution, Vol. 147, pp. 218-22, 2000.

[18] D. Chatterjee, A. Ghosh, "Transient stability assessment of power systems containing series and shunt compensators", IEEE Transactions on Power Systems, Vol. 22, pp. 1210-1220, 2007.

[19] P.R. Sharma, A. Kumar, N. Kumar, "Optimal location for shunt connected FACTS devices in a series compensated long transmission line", Turkish Journal of Electrical Engineering and Computer Sciences, Vol. 15, pp. 321-328, 2007.

[20] S. Panda, N.P. Padhy, "Optimal location and controller design of STATCOM for power system stability improvement using PSO", Journal of the Franklin Institute, Vol. 345, pp. 166-181, 2008.

[21] G. Wang, M. Zhang, X. Xu, C. Jiang, "Optimization of controller parameters based on the improved genetic algorithms", Proceedings of the 6th World Congress on Intelligence Control and Automation, pp. 3695-3698, 2006.

[22] D. Joshi, K.S. Sandhu, M.K. Soni, "Voltage control of self-excited induction generator using genetic algorithm", Turkish Journal of Electrical Engineering and Computer Sciences, Vol. 17, pp. 87-97, 2009.

[23] P.P. Narayana, M.A. Abdel-Moamen, B.J. Praveen-Kumar, "Optimal location and initial parameter settings of multiple TCSCs for reactive power planning using genetic algorithm", IEEE Power Engineering Society General Meeting, pp. 1110-1114, 2004.

[24] L. Ippolito, P. Siano, "Selection of optimal number and location of thyristor-controlled phase shifters using genetic based algorithms", IEE Proceedings - Generation Transmission and Distribution. Vol. 151, pp. 630-637, 2004.

[25] D. Radu, Y. Besanger, "A multi-objective genetic algorithm approach to optimal allocation of multi-type FACTS devices for power system security", Proceedings of the IEEE Future Power System Conference, 2006.

[26] S. Gerbex, R. Cherkaoui, A.J. Germond,, "Optimal location of multi-type FACTS devices in a power system by means of genetic algorithms", IEEE Transactions on Power Systems, Vol. 16, pp. 537-544, 2001.

[27] G.I. Rashed, H.I. Shaheen, S.J. Cheng, "Optimal location and parameter setting of TCSC by both genetic algorithm and particle swarm optimization", IEEE Conference on Industrial Electronics and Applications, pp. 1141-1147, 2007.

[28] M.A. Abido, "Analysis and assessment of STATCOM-based damping stabilizers for power system stability enhancement", Electric Power Systems Research, Vol. 73, pp. 177-185, 2005.

[29] S. Robak, "Robust SVC controller design and analysis for uncertain power systems", Control Engineering Practice, Vol. 17, pp. 1280-1290, 2009.

[30] H. Bevrani, T. Hiyama, H. Bevrani, "Robust PID based power system stabilizer: design and real-time implementation", Electrical Power and Energy Systems, Vol. 33, pp. 179-188, 2011.

[31] G. Shahgholian, P. Shafaghi, S. Moalem, M. Mahdavian, "Damping power system oscillations in single-machine infinite-bus power system using a STATCOM", Second International Conference on Computer and Electrical Engineering, pp. 130-134, 2009.

[32] D. Harikrishna, N.V. Srikanth, "Unified Philips-Heffron model of multi-machine power system equipped with PID damping controlled SVC for power oscillation damping", Annual IEEE India Conference, pp. 1-4, 2009.

[33] S. Panda, "Differential evolutionary algorithm for TCSC-based controller design", Simulation Modeling Practice and Theory, Vol. 17, pp. 1618-1634, 2009.

[34] L.J. Cai, I. Erlich, "Simultaneous coordinated tuning of PSS and FACTS damping controllers in large power systems", IEEE Transactions on Power Systems, Vol. 20, pp. 294-300, 2005.

[35] N. Li, Y. Xu, H. Chen, "FACTS-based power flow control in interconnected power systems", IEEE Transactions on Power Systems, Vol. 15, pp. 257-262, 2000.

[36] A.L Alam, M.A. Abido, "Parameter optimization of shunt FACTS controllers for power system transient stability improvement", IEEE Lausanne PowerTech, pp. 2012-2017, 2007.

[37] S. Panda, S.C. Swain, P.K. Rautray, R.K. Malik, G. Panda, "Design and analysis of SSSC-based supplementary damping controller", Simulation Modeling Practice and Theory, Vol. 18, pp. 1199-1213, 2010.

[38] S. Mishra, P.K. Dash, P.K. Hota, M. Tripathy, "Genetically optimized neuro-fuzzy IPFC for damping modal oscillations of power system", IEEE Transactions on Power Systems, Vol. 22, pp. 60-60, 2002.

[39] S. Panda, "Multi-objective evolutionary algorithm for SSSC-based controller design", Electric Power Systems Research, Vol. 79, pp. 937-944, 2009.